INTERNATIONAL JOURNAL FOR NUMERICAL METHODS IN FLUIDS
Int. J. Numer. Meth. Fluids 2008; **56**:1329–1336
Published online in Wiley InterScience (www.interscience.wiley.com). DOI: 10.1002/fld.1745

Numerical simulation of film cooling effectiveness on a flat plate

Homayoon Kanani[1], Mehrzad Shams[1,*,†], Reza Ebrahimi[1] and Taher Ahmadian[2,‡]

[1]*K.N. Toosi University of Technology, Faculty of Mechanical Engineering, Pardis St., Mollasadra St., Vanak Sq., Tehran, Iran*
[2]*Khuzestan Steel Company, 3rd Gate, 10 km Bandar Imam Khomeini Road, Ahwaz, Iran*

SUMMARY

Numerical simulation has been conducted to study film cooling effectiveness on a flat plate. Three-dimensional geometry was generated and the effects of blowing ratio and geometrical shape were studied. A cylindrical round, simple angle (CYSA) and laterally diffused, simple angle (LDSA) hole with a streamwise angle of 30° and spanwise angle of 0° were used. Hole length to diameter ratio ($L/D=4$) is constant for all geometries. Also the diameter of film cooling hole for different cooling holes at the entrance surface ($D=10$ mm) is constant. The blowing ratio ranges from 0.5 to 1.67, and the mainstream Reynolds number based on the mainstream velocity and hole diameter (Re_D) was 8563. Both local and lateral averaged values are presented. Results have a good correspondence with experimental data obtained by Yuen and Martinez-Botas (*Int. J. Heat Mass Transfer* 2003; **46**:221–235). The simulation results show that cooling hole shape affects film cooling effectiveness significantly. The LDSA hole decreases the momentum of jet flow at the exit area of the hole and avoids lift-off phenomenon. Counter-rotating vortex formed downstream of the hole is weaker for the LDSA hole and secondary flow is not powerful enough to disturb the jet flow structure next to the wall. Also the results show that the LDSA hole has a better lateral coverage due to the diffused shape of the hole and has a higher effectiveness value in a wider region on the wall. Copyright © 2008 John Wiley & Sons, Ltd.

Received 19 May 2007; Revised 12 December 2007; Accepted 12 December 2007

KEY WORDS: film cooling; single hole; computational fluid dynamics; flat plate

1. INTRODUCTION

Film cooling is commonly used to prevent thermal failure in turbine blades that could result from the operation in high temperature environment. Film cooling studies on a flat plate with cylindrical

*Correspondence to: Mehrzad Shams, K.N. Toosi University of Technology, Faculty of Mechanical Engineering, Pardis St., Mollasadra St., Vanak Sq., Tehran, Iran.
†E-mail: shams@kntu.ac.ir
‡Engineering Manager.

Contract/grant sponsor: Khuzestan Steel Company

holes have been carried out by Yuen and Martinez-Botas [1], Baldauf *et al.* [2] and Goldstein *et al.* [3]. Dittmar *et al.* [4] as well as Bell *et al.* [5] applied various film cooling configurations in order to study the film cooling effectiveness. Thole *et al.* [6] and Gritsch *et al.* [7] studied film cooling effectiveness for different geometries of hole. Their results show that expanded holes have better thermal protection of the surface downstream of the injection hole, particularly at high blowing ratios. Most numerical investigations of film cooling problems are based on the Reynolds-averaged Navier–Stokes equations. Garg and Gaugler [8] studied different cooling hole shapes numerically. They concluded that the shape of exit plane also affects heat transfer coefficient levels that were shown to differ by as much as 60% depending on the type of exit distribution used. Walters and Leylek [9] studied a row of cylindrical film cooling hole, and Hyams *et al.* [10] studied five different shapes of film cooling holes. Colban and Thole [11] evaluated the adiabatic and cooling performance of the cylindrical and fan-shaped holes on the endwall for a turbine blade. They concluded that fan-shaped holes are over cylindrical holes from both an aerodynamic and a thermal perspective. Gustafsson and Johansson [12] investigated film cooling using Reynolds stress models (RSM) and found them to be superior to a $k-\varepsilon$ or the SST $k-\omega$ models. In this study film cooling effectiveness has been investigated numerically on a flat plate including impingement chamber. The geometry of domain and all boundary conditions are similar to the experimental case study done by Yuen and Martinez-Botas [1].

2. GRID GENERATION

Figure 1(a) shows the geometry of the impingement and film cooling on a flat plate. While the size of duct of the mainstream is $360\,\text{mm} \times 114\,\text{mm} \times 1265\,\text{mm}$, the size of the path of the cooling stream is $100\,\text{mm} \times 230\,\text{mm} \times 100\,\text{mm}$. The diameter of cooling hole is 10 mm and length to diameter ratio is 4. The streamwise angle between the centreline of jet cooling hole and the mainstream flow is 30°. The zone which is distinguished with dotted box in Figure 1(a) includes impingement chamber and film cooling hole. The zone is presented in detail in Figure 1(b). The array of pipes located beneath the impingement chamber consists of 46 pipes positioned in staggered form (Figure 1(c)). Two kinds of configurations including cylindrical round, simple angle (CYSA) and lateral diffused, simple angle (LDSA) hole that have been studied in this paper are shown in Figure 1(d) and (e). As it is seen in Figure 1(e), the film cooling hole in LDSA hole is expanded on lateral side with taper angle of 14°. Unstructured grid with tetrahedral mesh elements was created for

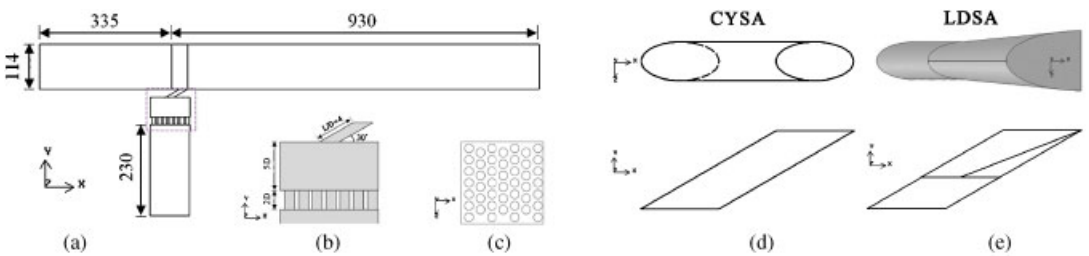

Figure 1. (a) The side view of geometry, unit: mm; (b) close view of the cooling hole and impingement chamber; (c) upside view of array of pipes; (d) CYSA; and (e) LDSA holes.

DOI: 10.1002/fld

film cooling hole, impingement chamber, impingement cooling pipes and coolant stream domain, while structured grid with hexahedral mesh elements was used for the mainstream duct. For every CFD calculation, a grid independence study has to be done to demonstrate that the calculated solution of the flow field is not dependent of the chosen mesh and the resolution of the mesh for the flow field is fine enough. For three-dimensional cases studied in this paper, the total number of grids for the mainstream is 364 800 and grid independence study has been done. In near wall region, the calculation mesh at the surfaces must be very fine, y^+ around 1, to assure the required resolution of the surface boundary layer. For accurate results the stainless steel sheet properties used in experimental apparatus [1] were considered in the simulation.

3. GOVERNING EQUATIONS

The flow and heat transfer problem for film cooling on a flat plate is modelled by the ensemble-averaged conservation equations of mass, momentum (three-dimensional incompressible Reynolds-averaged Navier–Stokes equation) and total energy for a thermally and perfect gas. Owing to the fact that the Mach number of the flow and temperature differences between cooling air and mainstream flow are low, the incompressible form of conservation equations was used. Abandoning the isotropic eddy-viscosity hypothesis, the RSM was used for turbulence modeling. The RSM equation was stated as follows:

$$\overline{u}_k \frac{\partial}{\partial x_k} R_{ij} = \frac{\partial}{\partial x_k}\left(\frac{\nu_t}{\sigma_k}\frac{\partial}{\partial x_k} R_{ij}\right) - \left[R_{ik}\frac{\partial \overline{u}_j}{\partial x_k} + R_{jk}\frac{\partial \overline{u}_i}{\partial x_k}\right] - C_1 \frac{\varepsilon}{k}\left[R_{ij} - \frac{2}{3}\delta_{ij}k\right] - C_2\left[P_{ij} - \frac{2}{3}\delta_{ij}P\right] - \frac{2}{3}\delta_{ij}\varepsilon \tag{1}$$

where $R_{ij} = \overline{u_i' u_j'}$ is the Reynolds stress tensor, $P_{ij} = -R_{ik}\partial \overline{u}_j/\partial x_k - R_{jk}\partial \overline{u}_i/\partial x_k$ is the turbulence production terms and $k = \frac{1}{2}\overline{u_i' u_i'}$ is the turbulent kinetic energy. The dissipation rate of turbulence is given by

$$\frac{\partial}{\partial x_i}(\rho \varepsilon u_i) = \frac{\partial}{\partial x_j}\left[\left(\mu + \frac{\mu_t}{\sigma_s}\right)\frac{\partial \varepsilon}{\partial x_j}\right] C_{\varepsilon 1}\frac{1}{2}\frac{\varepsilon}{k}P_{ii} - C_{\varepsilon 2}\rho\frac{\varepsilon^2}{k} \tag{2}$$

where $\mu_t = \rho C_\mu k^2/\varepsilon$ is the turbulent kinetic viscosity. The constants used in the above equations are $\sigma_s = 1.0$, $\sigma_k = 0.85$, $C_1 = 1.8$, $C_2 = 0.6$, $C_{\varepsilon 1} = 1.44$, $C_{\varepsilon 2} = 1.92$ and $C_\mu = 0.09$. Also, conduction equation is used for heat transfer modelling in the stainless steel sheet. A second-order upwind discretization scheme based on the control volume techniques is used to solve the governing integral equations for mass, momentum, energy and turbulence quantities defined above. The steady-state incompressible flows at a flat plate are studied numerically. SIMPLE algorithm is used for pressure–velocity coupling. In addition to simplification of boundary conditions and geometry model, the turbulence modelling approach can also have a significant impact on the accuracy of computational results.

DOI: 10.1002/fld

4. BOUNDARY CONDITIONS

The mainstream velocity was maintained at 13 m/s; therefore, the corresponding Reynolds number based on the hole diameter and mainstream velocity, Re_D, was 8563. The mainstream temperature and turbulence intensity were 293 K and 2.7%, respectively, where the cooling flow temperature at the inlet of coolant flow stream was 313 K and the turbulence intensity at the inlet boundary of coolant stream was set as 4%. Blowing ratio, $M=\rho_c u_c/\rho_\infty u_\infty$, is one of parameters that has a significant effect on the film cooling effectiveness, where ρ and u are the density and speed, respectively. Also subscript c and ∞ are the coolant and mainstream flow, respectively. The mass flow rate of coolant flow in each case study was obtained from the blowing ratio. In this work the blowing ratio set as 0.5, 0.67, 1.0, 1.33 and 1.67, where density ratio that was defined as the ratio between the density of cooling air and mainstream flow, was maintained at 0.92 according to the experimental data [1]. Flat plate was a stainless steel sheet with thickness of 0.0002 m and conductivity of 14.9 W/m K. Adiabatic wall condition was set at the bottom of this plate and all the other surfaces in the domain. All the above assumptions were considered according to the experimental work [1].

5. RESULTS

Film cooling effectiveness, $\eta=(T_{aw}-T_\infty)/(T_c-T_\infty)$, is a suitable parameter to investigate the cooling potential of the injected film without any heat flux into the wall, where T_{aw}, T_c and T_∞ are the temperature of the adiabatic wall, coolant injection flow and mainstream, respectively.

In Figure 2(a) the contour distribution of the film cooling effectiveness for a single 30° CYSA cooling hole is shown in the form of two-dimensional contours on the flat plate downstream of the cooling hole with blowing ratio ranges from 0.5 to 1.67, where the direction of mainstream flow as shown in Figure 2(a) is from left to right and the origin of the coordinate axis is positioned at the centre of the cooling hole. As the blowing ratio increases from 0.5 to 1.67, due to the lift-off phenomenon, the penetration of the cooling jet to the mainstream is increased and the film cooling effectiveness is decreased in both streamwise and spanwise directions. Spreading of film cooling extends in spanwise direction (z-direction) about three times of the hole diameter according to the experimental results [1, 3].

In Figure 2(b) the contour distribution of the film cooling effectiveness for LDSA configuration with the same inclined angle of CYSA configuration is shown. Because of larger exit area due to the lateral expanding of this shaped hole configuration, the coolant flow enters into the mainstream with a lower velocity (lower momentum). Therefore, lower penetration of injected flow caused by lower velocity occurs and coolant flow has a better coverage on the surface and it will be predictable that the effective region of film cooling for the LDSA configuration be bigger than CYSA configuration. If the momentum of the jet is big enough, it elevates from the plate. Less the elevation of the jet and therefore distance between the jet and plate, less the strength of the secondary flow. It increases the durability of the jet flow near the plate in the streamwise direction (x-direction). Also, the larger exit area of the LDSA hole leads to decrease in the jet velocity and reduces the height of the jet flow and extends the width of it over the plate. Temperature contour of CYSA and LDSA configurations at $z=0$ for blowing ratio of 0.5 are showed in Figures 3(a) and (b), respectively. The side view of the jet in Figure 3(a) indicates that the more penetration of the jet in CYSA configuration leads to increase in jet dispersion in the mainstream. As it is

DOI: 10.1002/fld

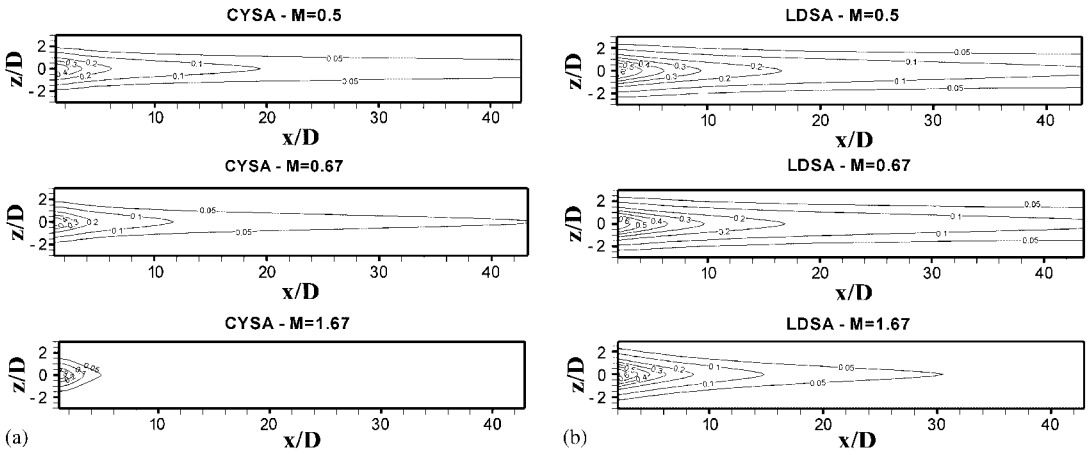

Figure 2. Contour distribution of the film cooling effectiveness for (a) CYSA and (b) LDSA configuration.

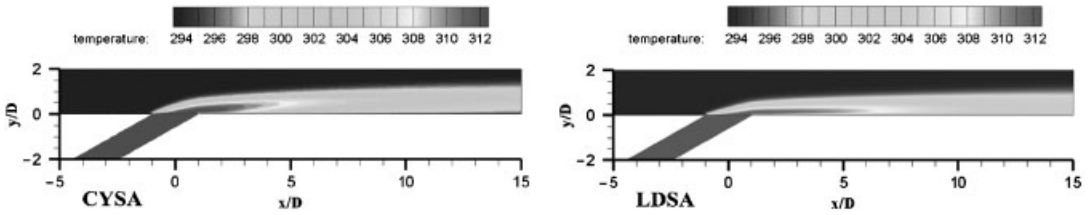

Figure 3. Side view of the jet for the CYSA and LDSA holes.

seen in Figure 3(b) the jet flow has a more flat shape for the LDSA hole compared with the CYSA. The large amount of the jet flow in the LDSA structure maintained in the vicinity of the wall and the weak counter-rotating vortex cannot disturb the cooling flow near the wall. The centreline effectiveness of CYSA configuration and experimental data for 30° film cooling hole is shown in Figure 4(a). The centreline effectiveness is decreased by increasing blowing ratio from 0.5 to 1.67, as observed. The numerical results have a good correspondence with experimental data except in regions near the cooling hole where the numerical results have a greater value than experimental data. Whereas generally the experimental data have uncertainties in the regions near the hole [13] and there are differences among them, also due to the 10% of uncertainties in the Yuen and Martinez-Botas [1] experimental study, the numerical error in the present work could be neglected. The centreline effectiveness of both CYSA and LDSA configurations has been shown in Figure 4(a) and (b). The expanding angle at the exit of the cooling hole will cause the cooling stream to remain attached on the wall by reducing the momentum with greater cross-section area and avoid the stream from lift-off. Lower momentum of the LDSA causes remarkable increasing of effectiveness in the same blowing ratio as expected. Velocity vectors have been shown in Figure 5(a) and (b) for both the CYSA and LDSA configurations in two cross-section planes (y–z), at $x/D=2$ and 6. Unlike CYSA configuration in which counter-rotating vortex leads to reduce film cooling performance, LDSA cooling hole prevents formation of these vortexes greatly; therefore,

DOI: 10.1002/fld

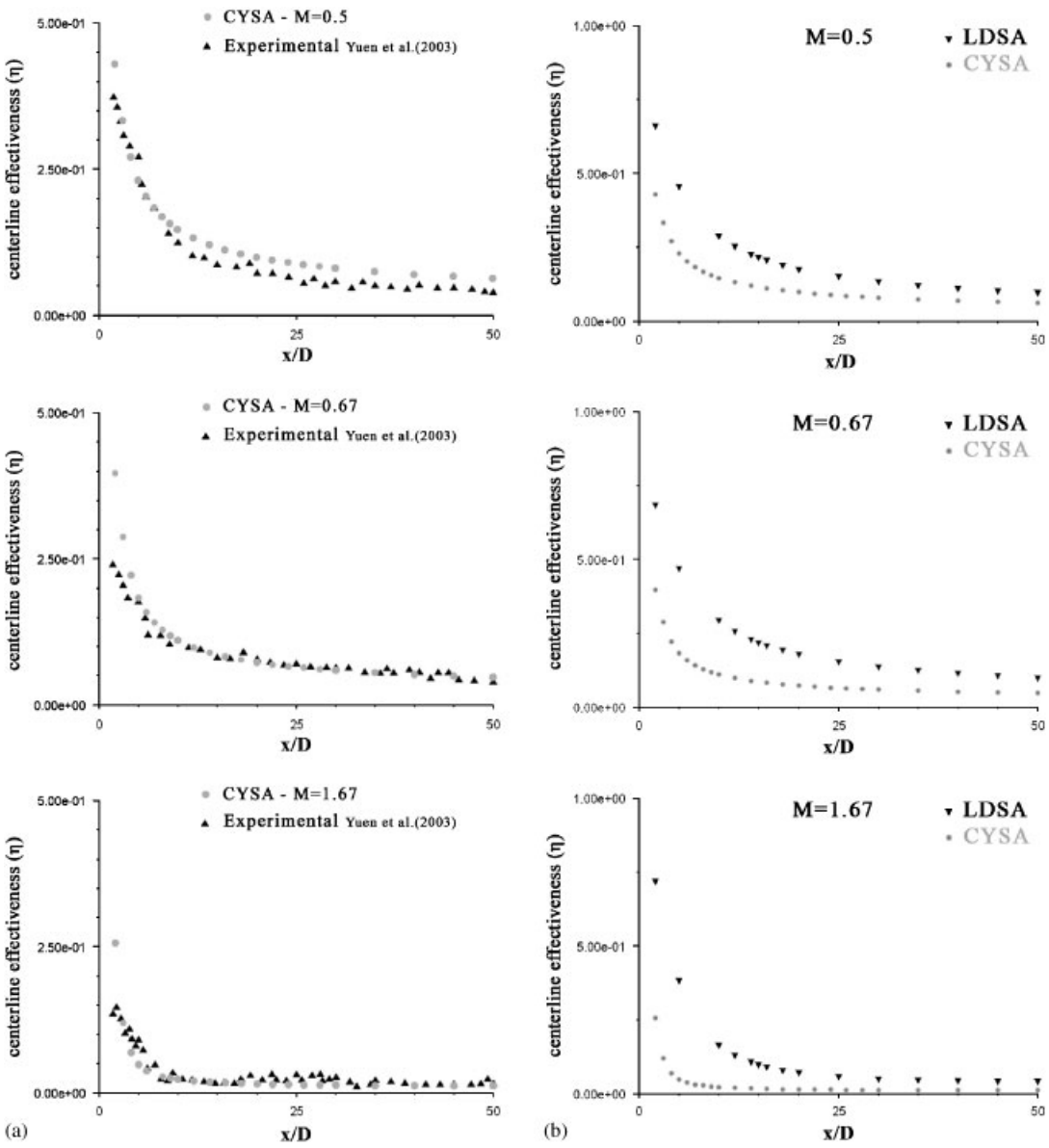

Figure 4. Centreline effectiveness for (a) CYSA and (b) LDSA 30° cooling hole.

the mainstream gas cannot flow beneath the cooling jet easily and lateral angle of this configuration causes excellent coverage of the coolant flow. It is seen that the size of velocity vectors for CYSA is larger than that for LDSA in same locations and the centre of vortex is closer to the centreline of cooling jet in CYSA configuration than that of LDSA. The velocity vectors indicate that in the LDSA type of cooling hole coolant flow is flatter and the distribution of injected flow is more

DOI: 10.1002/fld

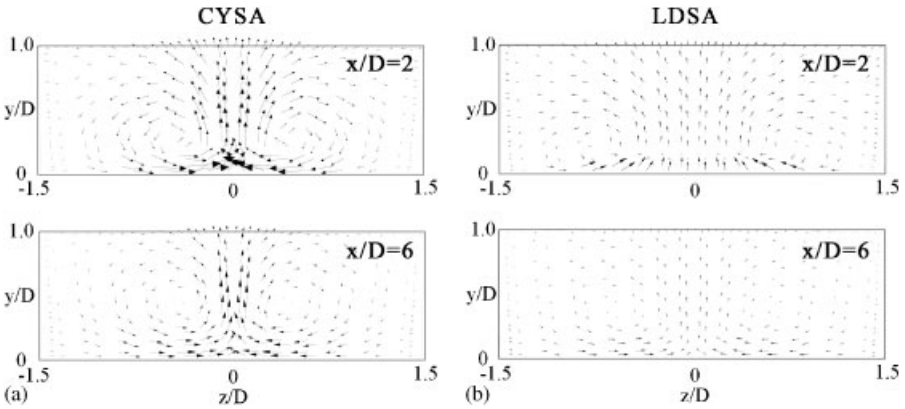

Figure 5. Velocity vectors for (a) CYSA and (b) LDSA cooling hole.

extended in spanwise direction (z-direction) than transverse direction (y-direction) in comparison with CYSA configuration.

6. CONCLUSION

Numerical simulation has been performed to investigate the film cooling effectiveness for three-dimensional cylindrical round, simple angle hole (CYSA) and lateral diffused, simple angle hole (LDSA) on a flat plate. The numerical results have been shown in the form of film cooling distribution on the test plate, centreline film cooling effectiveness in streamwise direction and velocity vectors in two spanwise planes for two different types of cooling holes. Main numerical simulation conclusions are: (1) For the CYSA configuration the more effective region ($\eta>0.2$) in streamwise direction does not extend beyond x/D of 6. This region extends about x/D of 16 for the LDSA hole. Also film cooling at high blowing ratios was not as effective as at low ratios for the CYSA cooling hole. For the LDSA hole, the varying of blowing ratio affects the centreline effectiveness considerably; however, it has a little effect on spreading of cooling jet in spanwise direction. Whereas the maximum value of effectiveness for the CYSA hole achieves blowing ratio of about 0.5, it is about 0.58 for the LDSA hole. (2) The shape of cooling hole plays an important role in the film cooling effectiveness. The LDSA cooling hole can reduce the momentum of cooling stream; therefore, this type of configuration has a better coverage of cooling flow on the surface of the test plate. Also the taper angle in the LDSA hole causes lateral spreading of the cooling jet. (3) In the region near the hole of the CYSA configuration, effective counter rotating vortex is formed and secondary flow causes film cooled flow move upward and reduces the film cooling effectiveness, whereas this vortex is very weak for the LDSA hole which causes the film cooled flow to stick around the flat plate and more effective film cooling happens.

ACKNOWLEDGEMENT

The support of Khuzestan Steel Company is gratefully acknowledged.

DOI: 10.1002/fld

REFERENCES

1. Yuen CHN, Martinez-Botas RF. Characteristics of a single round hole at various streamwise angles in a crossflow: part-I effectiveness. *International Journal of Heat and Mass Transfer* 2003; **46**:221–235.
2. Baldauf S, Schulz A, Wittig S. High resolution measurements of local heat transfer coefficients by discrete hole film cooling. *Journal of Turbomachinery* (ASME) 2001; **123**:758–765. Paper No. 99-GT-43.
3. Goldstein RJ, Jin P, Olson RL. Film cooling effectiveness and mass/heat transfer coefficient downstream of one row of discrete holes. *Journal of Turbomachinery* (ASME) 1999; **121**:225–232.
4. Dittmar J, Schulz A, Wittig S. Assessment of various film-cooling configurations including shaped and compound angle holes based on large-scale experiments. *Journal of Turbomachinery* (ASME) 2003; **125**:57–65.
5. Bell CM, Hamakawa H, Ligrani PM. Film cooling from shaped holes. *Journal of Heat Transfer* (ASME) 2000; **122**:224–232.
6. Thole K, Gritsch M, Schulz A, Wittig S. Flow field measurements for film cooling holes with expanded exits. *Journal of Turbomachinery* (ASME) 1998; **120**:327–336.
7. Gritsch M, Schulz A, Wittig S. Adiabatic wall effectiveness measurements of film-cooling holes with expanded exits. *Journal of Turbomachinery* (ASME) 1998; **120**:549–556.
8. Garg VK, Gaugler RE. Effect of velocity and temperature distribution at the hole exit on film cooling of turbine blades. *Journal of Turbomachinery* (ASME) 1997; **119**:343–351.
9. Walters DK, Leylek JH. A detailed analysis of film cooling physics: part I—streamwise injection with cylindrical holes. *Journal of Turbomachinery* (ASME) 2000; **122**:102–112.
10. Hyams D, McGovern K, Leylek J. A detailed analysis of film cooling physics: part III streamwise injection with shaped holes. *Journal of Turbomachinery* (ASME) 2000; **122**:122–132.
11. Colban W, Thole K. Influence of hole shape on the performance of a turbine vane endwall film-cooling scheme. *International Journal of Heat and Fluid Flow* 2007; **28**:341–356.
12. Gustafsson KMB, Johansson TG. Numerical simulation of effusion cooling with comparisons to experimental data. *Progress in Computational Fluid Dynamics* 2006; **6**:101–109.
13. Bubb J. The influence of pressure ratio on film cooling performance of a turbine blade. *Master Thesis in Mechanical Engineering*, Blacksburg, Virginia, 1999.

DOI: 10.1002/fld